

Supplementary Information

Giant electrostrain accompanying structural evolution in lead-free NBT-based piezoceramics

Xing Liu^a, Saidong Xue^b, Feng Li^a, Jinpeng Ma^b, Jiwei Zhai^{a,*}, Bo Shen^a, Feifei Wang^b, Xiangyong Zhao^b, Haixue Yan^{c,*}

^a*Key laboratory of Advanced Civil Engineering Materials of Ministry of Education, Functional Materials Research Laboratory, School of Materials Science & Engineering, Tongji University, 4800 Caoan Road, Shanghai 201804, China*

^b*Key Laboratory of Optoelectronic Material and Device, Department of Physics, Shanghai Normal University, Shanghai, 200234, China.*

^c*School of Engineering and Materials Science, Queen Mary University of London, Mile End Road, London E1 4NS, UK.*

*Corresponding authors:

E-mail addresses: apzhai@tongji.edu.cn (J. Zhai); h.x.yan@qmul.ac.uk (H. Yan)

Tel.: +86 21 69584759; fax: +86 21 69584759

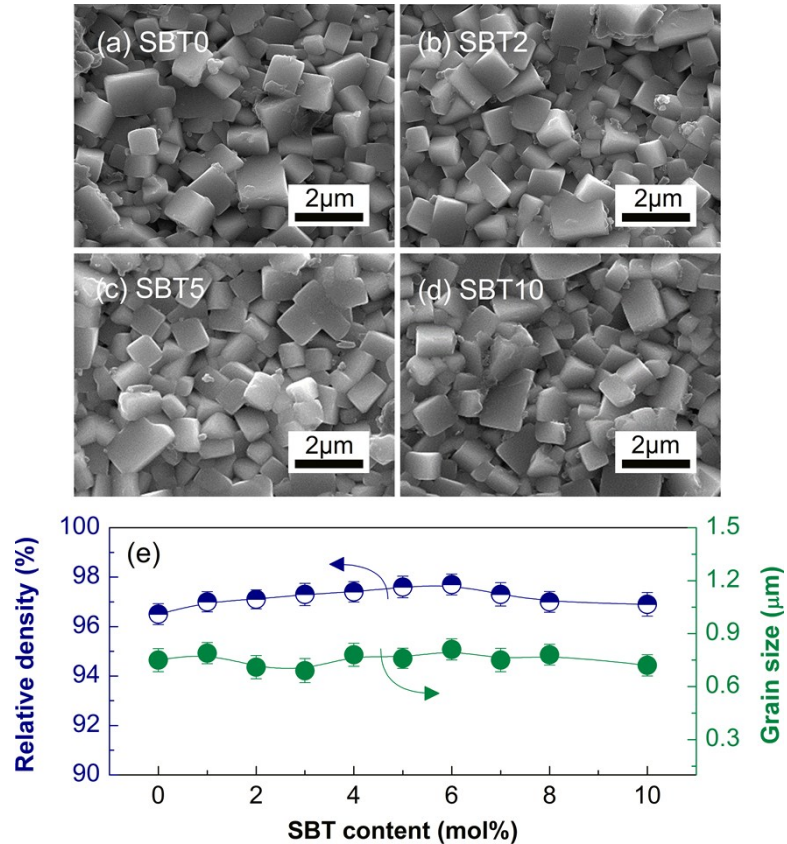


Fig. S1 SEM morphologies of SBT0 (a), SBT2 (b), SBT5 (c) and SBT10 (d) ceramics. The relative density and grain size as a function of SBT content (e).

Fig. S1(a)-(d) show the SEM micrographs of SBT0, SBT2, SBT5 and SBT10 samples, respectively. Fig. S1(e) provides the relative densities and grain size of all samples. All the synthesized ceramics present dense and homogeneous microstructure. The relative densities are ~97 % for all samples, and the average grain size calculated by the linear-intercept method is ~0.75 μm.

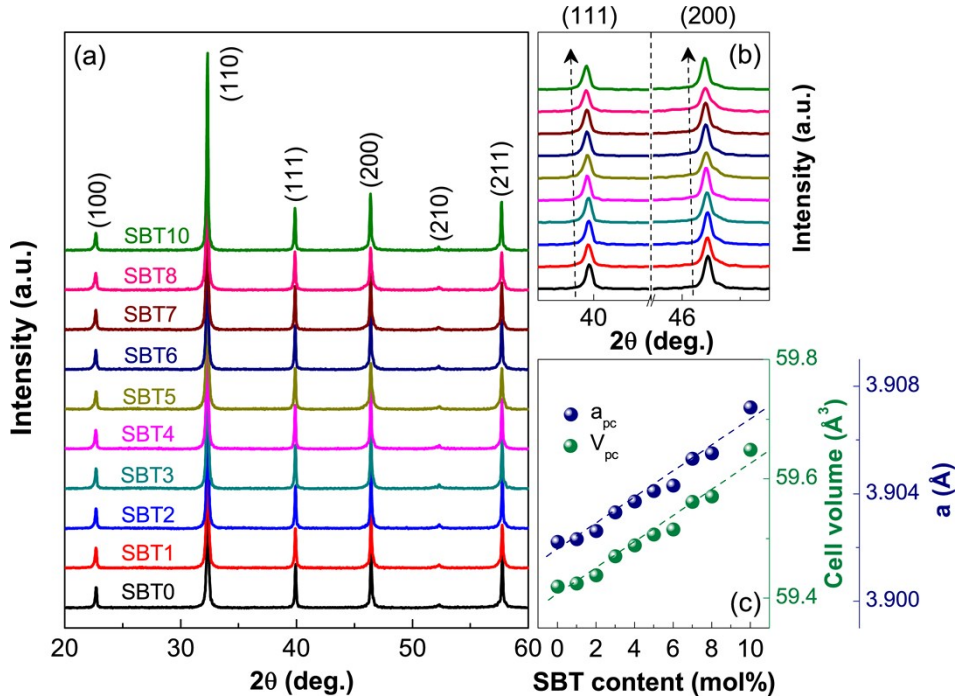


Fig. S2 X-ray diffraction patterns of SBT0-SBT10 samples (a); enlarged (111) and (200) diffraction peaks (b); the variation of lattice parameter a_{pc} and cell volume V_{pc} as a function of SBT content (c).

Fig. S2(a) shows the XRD patterns of all samples, and the locally magnified (111) and (200) characteristic diffraction peaks are shown in Fig. S2(b). The lattice parameter a_{pc} and cell volume V_{pc} as a function of SBT content are shown in Fig. S2(c). It indicates that desired pure perovskite phases are formed for compositions up to SBT10. All compositions exhibit pseudocubic phase structure, featured by the sharp and center-symmetric diffraction peaks, suggesting the absence of average distortion. Moreover, the diffraction peaks shift to lower angles (Fig. S2(b)), which is indicative of a slight lattice expansion. This is due to the fact that the ionic radii of Sr²⁺ is larger than that of Bi³⁺ and Na⁺ (CN=12, $R_{\text{Sr}}^{2+}=1.44$ Å, $R_{\text{Bi}}^{3+}=1.36$ Å, $R_{\text{Na}}^{+}=1.39$ Å).¹

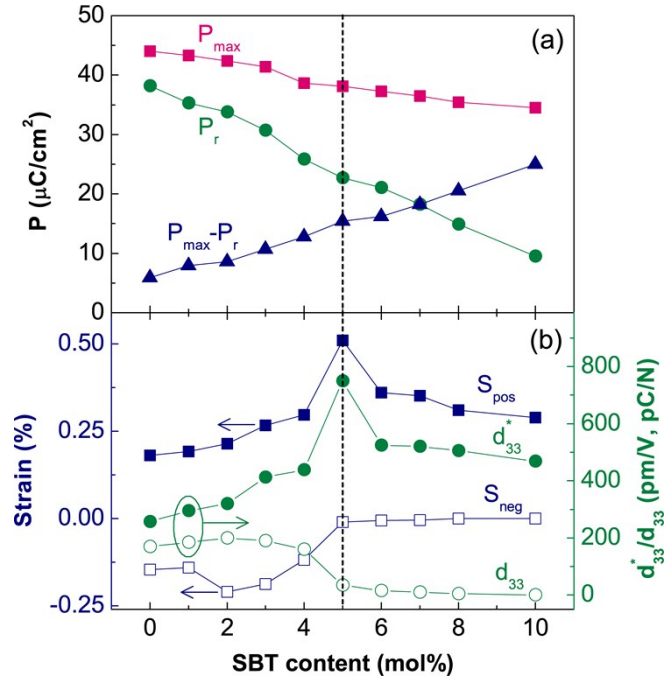


Fig. S3 The maximum polarization (P_{\max}), remanent polarization (P_r), the difference between them ($P_{\max}-P_r$) (a), positive strain (S_{pos}), negative strain (S_{neg}), large-signal piezoelectric constant (d_{33}^*) and small-signal piezoelectric constant (d_{33}) (b) with varying the SBT content.

Fig. S3 summarizes the polarization and strain parameters measured at 6 kV/mm and 10 Hz of all samples, including maximum polarization (P_{\max}), remanent polarization (P_r), the difference between them ($P_{\max}-P_r$), positive strain (S_{pos}), negative strain (S_{neg}), large-signal piezoelectric constant (d_{33}^*) and small-signal piezoelectric constant (d_{33}). The d_{33}^* value was calculated by the average unipolar strain per unit of electric field: $d_{33}^* = S_{\max}/E$. It can be seen that the polarization parameters exhibit a smooth change with SBT content, indicating a gradual loss of long-range ferroelectricity.² Such phenomenon is different from the reported incipient NBT ceramics, for which the polarization values always decrease sharply at ferroelectric-relaxor phase boundary.^{2,3} This can be attributed to the introduced extrinsic local defects: the local defects can act as the seed for the growth of ferroelectric domains and can also facilitate the polarization development since they possess the lowest energy barrier.^{4,5} The d_{33} and S_{neg} values, which are closely related to the domain back-switching,² reduce sharply at SBT5 composition. Furthermore, the S_{pos} and d_{33}^* values reach as high as 0.51 % and 750 pm/V at SBT5 composition. Such high recoverable strain is due to a field-induced relaxor-ferroelectric phase transformation.²

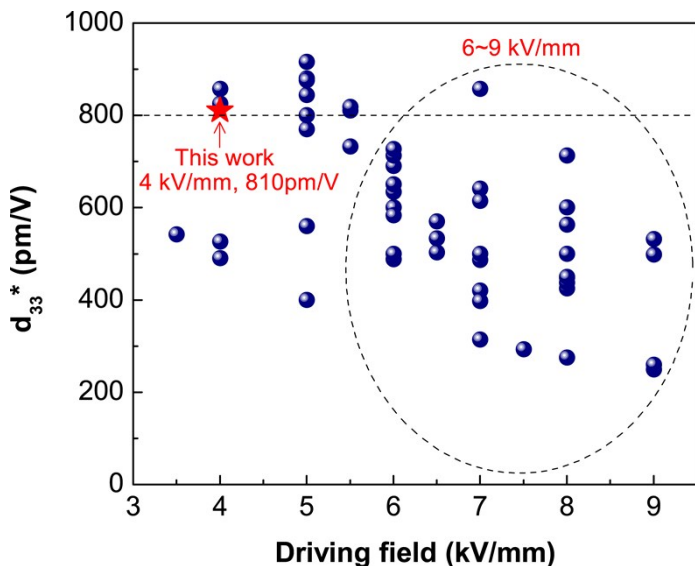


Fig. S4 Comparison of d_{33}^* values and driving fields for SBT5 sample and other NBT-based actuator ceramics.⁶⁻⁵¹

Fig. S4 presents the comparison of d_{33}^* values and driving fields for SBT5 sample and other NBT-based actuator ceramics.⁶⁻⁵¹ It can be seen that a relatively high external field of 6~9 kV/mm is needed to trigger the large strain in most NBT-based incipient ceramics, of which the d_{33}^* values are usually below 800 pm/V. The current SBT5 sample possesses a giant d_{33}^* value of 810 pm/V at a low field of 4 kV/mm. Via deliberately introducing the local defects, the activating field of SBT5 critical composition is significantly reduced as compared with other NBT-based systems, while the strain property can still reach a high level. The excellent piezoelectric strain performance makes SBT5 promising in applications of actuators and high-precision positioning devices.

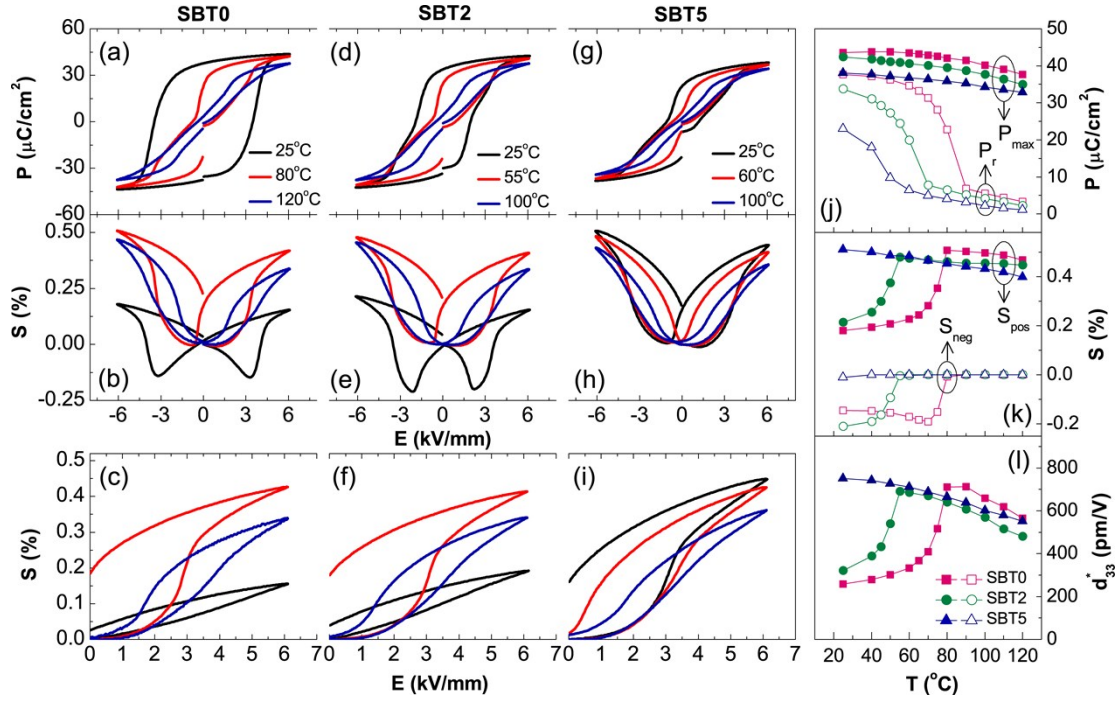


Fig. S5 The P - E hysteresis loops, bipolar and unipolar S - E curves of SBT0 (a)-(c), SBT2 (d)-(f) and SBT5 (g)-(i) samples measured at elevated temperatures. The temperature dependence of P_{\max} and P_r (j), S_{pos} and S_{neg} (k), and d_{33}^* (l) values for SBT0, SBT2 and SBT5 samples.

The temperature dependent polarization and strain measurements of SBT0, SBT2 and SBT5 samples were also carried out, as shown in Fig. S5. For SBT0 and SBT2 samples, the long-range ferroelectricity is significantly disrupted at their T_{FR} , accompanied by the reduction of P_r values and enhancement of S_{pos} and d_{33}^* values.¹⁸ However, the polarization and strain parameters of SBT5 sample decrease continuously with increasing temperature, because this composition locates at ferroelectric-relaxor phase boundary in the studied system.¹⁸ Furthermore, S_{pos} and d_{33}^* values of SBT5 sample vary less than 11 % up to 80 °C, and can still reach as high as 0.4 % and 552 pm/V at 120 °C, which is favorable for practical actuator applications. The excellent thermal stability of SBT5 sample is possibly due to a highly competitive free energy between relaxor and ferroelectric phases coexisting over a wide temperature range.¹⁸

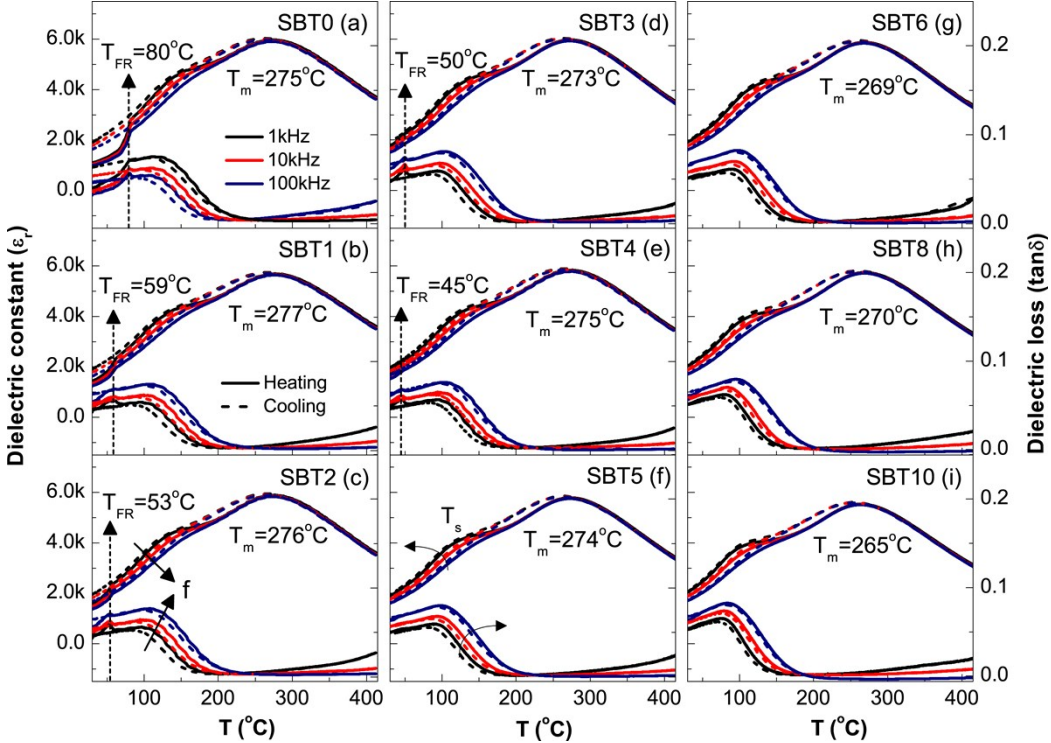


Fig. S6 Temperature dependence of dielectric constant (ϵ_r) and loss tangent ($\tan\delta$) of poled SBT0-SBT10 samples measured at 1, 10 and 100 kHz. The heating and cooling rate is set as $2\text{ }^{\circ}\text{C}/\text{min}$.

Fig. S6 summarizes the temperature dependence of dielectric constant (ϵ_r) and loss tangent ($\tan\delta$) of poled SBT0-SBT10 samples measured at 1, 10 and 100 kHz during the heating (solid lines) and cooling (dashed lines) processes. The heating and cooling rate is set as $2\text{ }^{\circ}\text{C}/\text{min}$. Compared to the cooling data (unpoled), a distinct dielectric anomaly at T_{FR} can be observed for poled SBT0-SBT4 samples. The T_{FR} decreases from $80\text{ }^{\circ}\text{C}$ for SBT0 sample, to $45\text{ }^{\circ}\text{C}$ for SBT4 sample, and disappears for SBT5-SBT10 samples. This clearly indicates a composition induced ferroelectric-relaxor phase transition.¹⁸ The SBT5 is considered as the critical transition composition. However, the T_m of all compositions is around $270\text{ }^{\circ}\text{C}$ and exhibits no obvious changes.

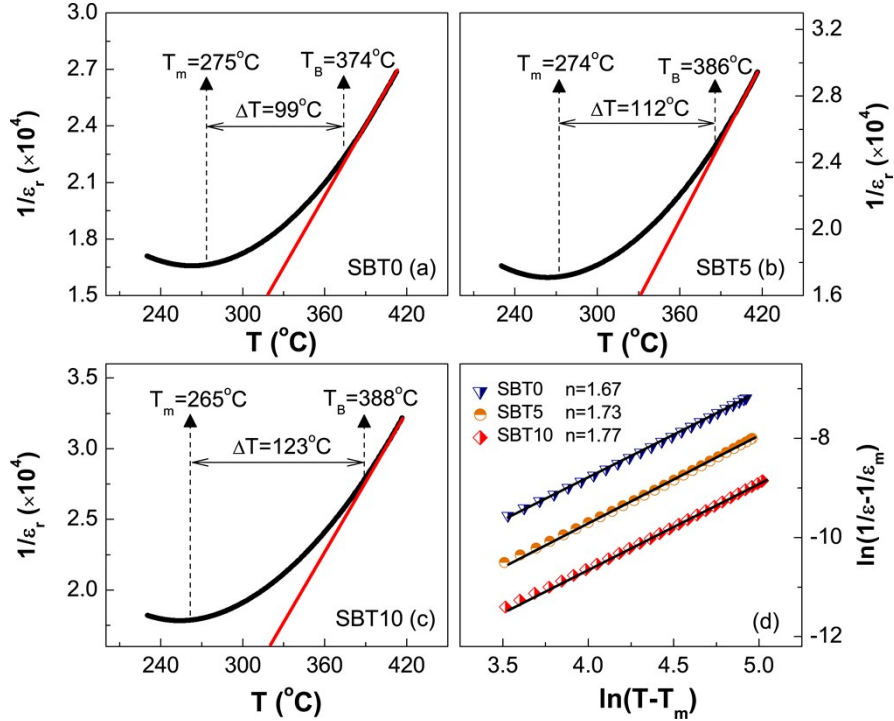


Fig. S7 The dielectric constant above T_m fitted by the modified Curie-Weiss law and quadratic law for SBT0, SBT5 and SBT10 compositions.

Fig. S7(a)-(d) show the linear fitting of dielectric constant (1 kHz) above T_m for SBT0, SBT5 and SBT10 samples by the Curie-Weiss law and quadratic law.⁵² The deviation degree ($\Delta T = T_B - T_m$) from the Curie-Weiss law is 99 °C, 112 °C and 123 °C for SBT0, SBT5 and SBT10 samples, respectively. The diffuseness factor (n) is 1.67, 1.73 and 1.77 for SBT0, SBT5 and SBT10 samples, respectively. Thus the SBT modification enhances the relaxor degree and favors a more disordered structure.⁵²

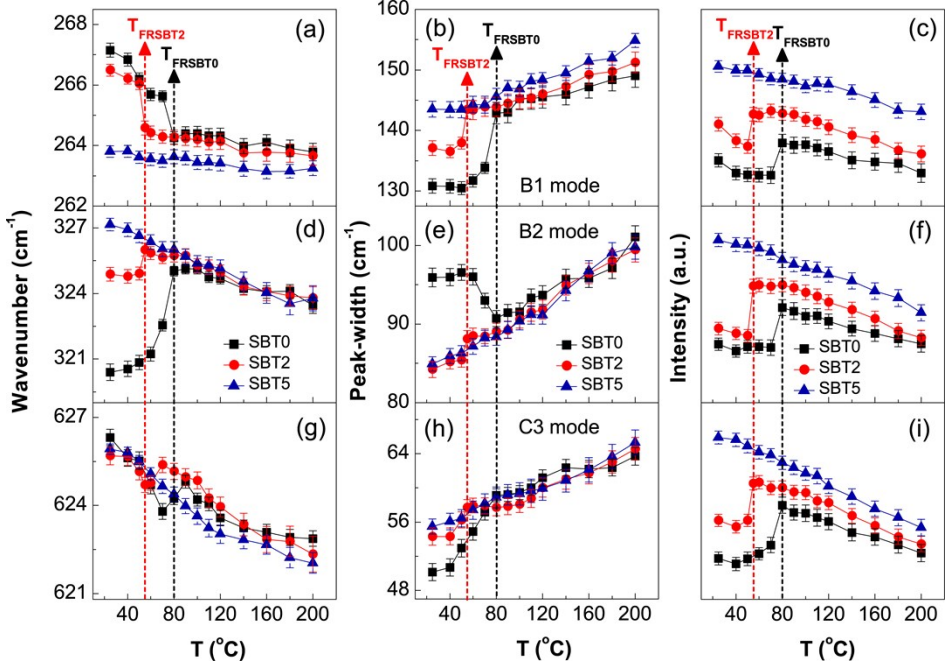


Fig. S8 The wavenumber, peak-width and Raman intensity of B_1 (a)-(c), B_2 (d)-(f) and C_3 (g)-(i) modes as a function of temperature for SBT0, SBT2 and SBT5 samples. The T_{FR} of SBT0 and SBT2 samples marked as the dashed lines is also provided.

The temperature dependent Raman spectra of SBT0, SBT2 and SBT5 samples were corrected by the Bose-Einstein population factor and decomposed into the Lorentzian-shaped peaks.⁵³ Then the detailed variations of Raman modes with increasing temperature can be obtained. Fig. S8 summarizes the temperature dependence of wavenumber, peak-width and Raman intensity of B_1 , B_2 and C_3 modes for poled SBT0, SBT2 and SBT5 samples. A discontinuous change occurs near T_{FR} for SBT0 and SBT2 samples, especially an abrupt increase of Raman intensity near the transitional temperature, suggesting a temperature induced ferroelectric-relaxor transition on a local scale.⁵⁴ However, the B_1 , B_2 and C_3 modes of SBT5 sample only experience successive peak softening accompanied by the peak broadening and reduction in intensity with increasing temperature, indicating the enhanced structural disorder with no phase transitions.⁵⁵ Such phenomenon is similar to that of polarization and strain measurements aforementioned, and the SBT modification can effectively reduce the T_{FR} .

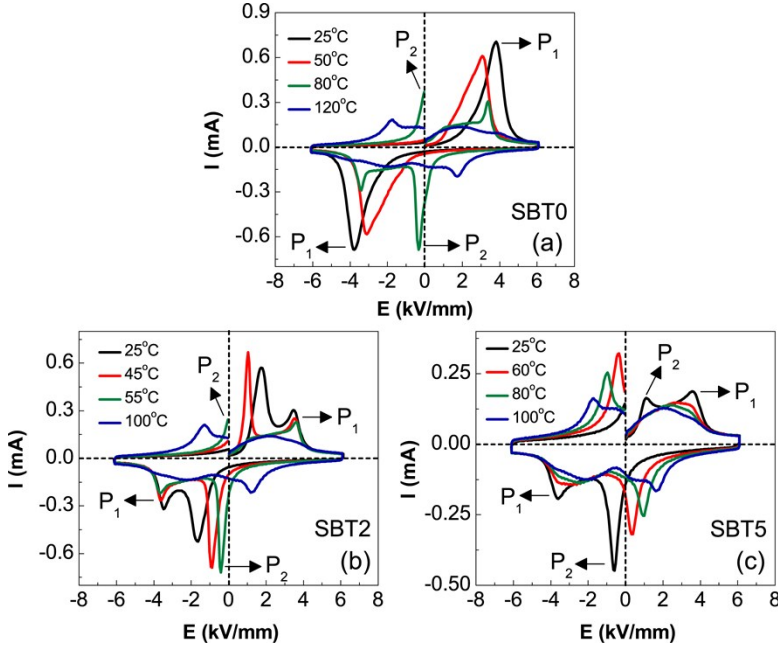


Fig. S9 The I - E hysteresis loops of SBT0 (a), SBT2 (b) and SBT5 (c) samples measured at different temperatures.

Fig. S9(a)-(c) show the I - E hysteresis loops measured at different temperatures for SBT0, SBT2 and SBT5 samples, respectively. The SBT0 sample exhibits two sharp current peaks (denoted by P_1) at RT, indicating the domain switching behavior of normal ferroelectrics.⁵⁶ However, another two peaks (denoted by P_2) locate at lower-field region can be observed for SBT2 sample at RT, suggesting the presence of relaxor phase and a two-step polarization reversal processes during electric loading or unloading: from ferroelectric to relaxor at P_2 and then from relaxor to ferroelectric at P_1 , correspondingly accompanied with the disruption and re-establishment of long-range polar domains.^{56,57} Moreover, the P_2 peaks move to zero field at T_{FR} for SBT0 and SBT2 samples, similar to that of SBT5 sample at RT. This indicates that the high-temperature relaxor phase is stabilized at RT by SBT modification, and SBT5 composition locates at the ferroelectric-relaxor phase boundary.⁵⁶ Above T_{FR} , the P_2 peaks of all samples shift to the higher field region in second and fourth quadrant, while the P_1 peaks smear progressively, which can be attributed to the increasing relaxor phase content and the weakening of ferroelectricity at high temperatures.^{55,56}

References

- 1 R.D. Shannon, *Acta Cryst.*, 1976, **A32**, 751.
- 2 W. Jo, T. Granzow, E. Aulbach, J. Rödel and D. Damjanovic, *J. Appl. Phys.*, 2009, **105**, 094102.
- 3 W. Jo, R. Dittmer, M. Acosta, J. Zang, C. Groh, E. Sapper, K. Wang and J. Rödel, *J. Electroceram.*, 2012, **29**, 71.
- 4 S. Jesse, B. J. Rodriguez, S. Choudhury, A. P. Baddorf, I. Vrejoiu, D. Hesse, M. Alexe, E. A. Eliseev, A. N. Morozovska, J. Zhang, L. Q. Chen and S. V. Kalinin, *Nat. Mater.*, 2008, **7**, 209.
- 5 D. Viehland and J. F. Li, *J. Appl. Phys.*, 2001, **90**, 2995.
- 6 J. Rödel, K. G. Webber, R. Dittmer, W. Jo, M. Kimura and D. Damjanovic, *J. Eur. Ceram. Soc.*, 2015, **35**, 1659.
- 7 A. B. Kounga, S. T. Zhang, W. Jo, T. Granzow and J. Rödel, *Appl. Phys. Lett.*, 2008, **92**, 222902.
- 8 S. T. Zhang, A. B. Kounga, E. Aulbach, H. Ehrenberg and J. Rödel, *Appl. Phys. Lett.*, 2007, **91**, 112906.
- 9 H. S. Han, W. Jo, J. K. Kang, C. W. Ahn, I. W. Kim, K. K. Ahn and J. S. Lee, *J. Appl. Phys.*, 2013, **113**, 154102.
- 10 R. A. Malik, A. Hussain, A. Zaman, A. Maqbool, J. U. Rahman, T. K. Song, W. J. Kim and M. H. Kim, *RSC Adv.*, 2015, **5**, 96953.
- 11 Y. Hiruma, Y. Imai, Y. Watanabe, H. Nagata and T. Takenaka, *Appl. Phys. Lett.*, 2008, **92**, 262904.
- 12 W. Bai, Y. Bian, J. Hao, B. Shen and J. Zhai, *J. Am. Ceram. Soc.*, 2013, **96**, 246.
- 13 Y. Hiruma, H. Nagata and T. Takenaka, *Appl. Phys. Lett.*, 2009, **95**, 052903.
- 14 F. Li, R. Zuo, D. Zheng and L. Li, *J. Am. Ceram. Soc.*, 2015, **98**, 811.

- 15 J. U. Rahman, A. Hussain, A. Maqbool, T. K. Song, W. J. Kim, S. S. Kim and M. H. Kim, *Curr. Appl. Phys.*, 2014, **14**, 331.
- 16 K. T. P. Seifert, W. Jo and J. Rödel, *J. Am. Ceram. Soc.*, 2010, **93**, 1392.
- 17 A. Ullah, C. W. Ahn, A. Ullah and I. W. Kim, *Appl. Phys. Lett.*, 2013, **103**, 022906.
- 18 K. Wang, A. Hussain, W. Jo and J. Rödel, *J. Am. Ceram. Soc.*, 2012, **95**, 2241.
- 19 H. S. Han, W. Jo, J. Rödel, I. K. Hong, W. P. Tai and J. S. Lee, *J. Phys.: Condens. Matter.*, 2012, **24**, 365901.
- 20 G. Dong, H. Fan, J. Shi and M. Li, *J. Am. Ceram. Soc.*, 2015, **98**, 1150.
- 21 A. Zaman, A. Hussain, R. A. Malik, A. Maqbool, S. Nahm and M. H. Kim, *J. Phys. D: Appl. Phys.*, 2016, **49**, 175301.
- 22 Q. Yao, F. Wang, F. Xu, C. M. Leung, T. Wang, Y. Tang, X. Ye, Y. Xie, D. Sun and W. Shi, *ACS Appl. Mater. Interfaces.*, 2015, **7**, 5066.
- 23 D. S. Yin, Z. H. Zhao, Y. J. Dai, Z. Zhao, X. W. Zhang and S. H. Wang, *J. Am. Ceram. Soc.*, 2016, **99**, 2354.
- 24 A. Ullah, R. A. Malik, A. Ullah, D. S. Lee, S. J. Jeong, J. S. Lee, I. W. Kim and C. W. Ahn, *J. Eur. Ceram. Soc.*, 2014, **34**, 29.
- 25 A. Maqbool, A. Hussain, R. A. Malik, J. U. Rahman, A. Zaman, T. K. Song, W. J. Kim and M. H. Kim, *Mater. Sci. Eng. B*, 2015, **199**, 105.
- 26 J. Chen, Y. Wang, Y. Zhang, Y. Yang and R. Jin, *J. Eur. Ceram. Soc.*, 2017, **37**, 2365.
- 27 K. N. Pham, A. Hussain, C. W. Ahn, I. W. Kim, S. J. Jeong and J. S. Lee, *Mater. Lett.*, 2010, **64**, 2219.
- 28 J. Shi, H. Fan, X. Liu and Q. Li, *J. Eur. Ceram. Soc.*, 2014, **34**, 3675.
- 29 L. Wu, B. Shen, Q. Hu, J. Chen, Y. Wang, Y. Xia, J. Yin and Z. Liu, *J. Am. Ceram. Soc.*, 2017, **100**, 4670.
- 30 R. A. Malik, J. K. Kang, A. Hussain, C. W. Ahn, H. S. Han and J. S. Lee, *Appl. Phys. Express.*,

2014, **7**, 061502.

- 31 A. Ullah, M. Alam, A. Ullah, C. W. Ahn, J. S. Lee, S. Cho and I. W. Kim, *RSC Adv.*, 2016, **6**, 63915.
- 32 A. Ullah, A. Ullah, I. W. Kim, D. S. Lee, S. J. Jeong and C. W. Ahn, *J. Am. Ceram. Soc.*, 2014, **97**, 2471.
- 33 Y. Li, F. Wang, X. Ye, Y. Xie, Y. Tang, D. Sun, W. Shi, X. Zhao and H. Luo, *J. Am. Ceram. Soc.*, 2014, **97**, 3615.
- 34 F. Wang, M. Xu, Y. Tang, T. Wang, W. Shi and C. M. Leung, *J. Am. Ceram. Soc.*, 2012, **95**, 1955.
- 35 P. Jaita, A. Watcharapasorn, N. Kumar, S. Jiansirisomboon and D. P. Cann, *J. Am. Ceram. Soc.*, 2016, **99**, 1615.
- 36 T. H. Dinh, J. K. Kang, J. S. Lee, N. H. Khansur, J. Daniels, H. Y. Lee, F. Z. Yao, K. Wang, J. F. Li, H. S. Han and W. Jo, *J. Eur. Ceram. Soc.*, 2016, **36**, 3401.
- 37 T. Li, X. Lou, X. Ke, S. Cheng, S. Mi, X. Wang, J. Shi, X. Liu, G. Dong, H. Fan, Y. Wang, X. Tan, *Acta Mater.*, 2017, **128**, 337.
- 38 V. Q. Nguyen, H. S. Han, K. J. Kim, D. D. Dang, K. K. Ahn and J. S. Lee, *J. Alloy. Compd.*, 2012, **511**, 237.
- 39 R. A. Malik, A. Hussain, A. Maqbool, A. Zaman, C. W. Ahn, J. U. Rahman, T. K. Song, W. J. Kim and M. H. Kim, *J. Am. Ceram. Soc.*, 2015, **98**, 3842.
- 40 J. Hao, Z. Xu, R. Chu, W. Li, J. Du and G. Li, *J. Phys. D: Appl. Phys.*, 2015, **48**, 472001.
- 41 R. Cheng, Z. Xu, R. Chu, J. Hao, J. Du and G. Li, *J. Eur. Ceram. Soc.*, 2016, **36**, 489.
- 42 W. Bai, F. Liu, P. Li, B. Shen, J. Zhai and H. Chen, *J. Eur. Ceram. Soc.*, 2015, **35**, 3457.
- 43 Y. Hiruma, H. Nagata and T. Takenaka, *J. Appl. Phys.*, 2008, **104**, 124106.
- 44 J. Hao, B. Shen, J. Zhai and H. Chen, *J. Am. Ceram. Soc.*, 2014, **97**, 1776.
- 45 J. Hao, W. Bai, W. Li, B. Shen and J. Zhai, *J. Mater. Res.*, 2012, **27**, 2943.

- 46 W. Bai, D. Chen, Y. Huang, P. Zheng, J. Zhong, M. Ding, Y. Yuan, B. Shen, J. Zhai and Z. Ji, *Ceram. Int.*, 2016, **42**, 7669.
- 47 W. Bai, D. Chen, Y. Huang, B. Shen, J. Zhai and Z. Ji, *J. Alloy. Compd.*, 2016, **667**, 6.
- 48 W. Bai, L. Li, W. Li, B. Shen, J. Zhai and H. Chen, *J. Am. Ceram. Soc.*, 2014, **97**, 3510.
- 49 Y. J. Dai, S. S. He, X. Lao and S. Z. Zhang, *J. Am. Ceram. Soc.*, 2014, **97**, 1283.
- 50 X. Liu, H. Guo and X. Tan, *J. Eur. Ceram. Soc.*, 2014, **34**, 2997.
- 51 H. Sun, X. Wu, D. F. Peng and K. W. Kwok, *ACS Appl. Mater. Interfaces.*, 2017, **9**, 34042.
- 52 K. Datta, P. A. Thomas and K. Roleder, *Phys. Rev. B*, 2010, **82**, 224105.
- 53 N. Waeselmann, B. Mihailova, B. J. Maier, C. Paulmann, M. Gospodinov, V. Marinova and U. Bismayer, *Phys. Rev. B*, 2011, **83**, 214104.
- 54 D. Schütz, M. Deluca, W. Krauss, A. Feteira, T. Jackson and K. Reichmann, *Adv. Funct. Mater.*, 2012, **22**, 2285.
- 55 X. Liu, F. Li, P. Li, J. Zhai, B. Shen and B. Liu, *J. Eur. Ceram. Soc.*, 2017, **37**, 4585.
- 56 Y. Ehara, N. Novak, S. Yasui, M. Itoh and K. G. Webber, *Appl. Phys. Lett.*, 2015, **107**, 262903.
- 57 H. Guo, X. Liu, F. Xue, L. Q. Chen, W. Hong, X. Tan, *Phys. Rev. B*, 2016, **93**, 174114.